Characteristics of layered occurrence ratio of polar mesosphere summer echoes observed by EISCAT VHF 224MHz Radar

5   Shucan Ge[1], Hailong Li[1], Tong Xu[2], Mengyan Zhu[2], Maoyan Wang[1], Lin Meng[1]

[1]School of Electronic Science and Engineering, University of Electronic Science and Technology of China, 610054, Chengdu, China

[2]National Key Laboratory of Electromagnetic Environment, China Research Institute of Radiowave Propagation, 266107, Qingdao, China

10   *Correspondence to*: Hailong Li (hailong703@163.com)

Abstract. Polar Mesosphere Summer Echoes (PMSE) are strong radar echoes observed in polar mesopause during local summer. Measurements of layered PMSE observed by the European Incoherent Scatter Scientific Association Very high frequency (EISCAT VHF) radar from 2004 to 2015 in the latest

15   solar cycle, can be used to study the variations of PMSE occurrence ratio (OR). The seasonal variation of PMSE mono-, double- and tri-layer occurrence ratio was analyzed, and there is different seasonal behavior. A method was given to calculate the PMSE mono-, double- and tri-layer occurrence ratio under different electron density threshold conditions. In addition, the correlation between PMSE layered occurrence ratios and solar 10.7 cm flux index (F10.7), and the correlation between PMSE layered

20   occurrence ratios and geomagnetic K index were analyzed respectively in this study. It can be obtained that PMSE mono-, double- and tri-layer OR are positively correlated with the K index. The correlation coefficient between PMSE mono- and double-layer OR and F10.7 is weak, and the PMSE tri-layer OR has a negative correlation with F10.7.

Keywords: Polar Mesosphere Summer Echoes; European Incoherent Scatter Scientific Association Very

25   high frequency Radar; solar 10.7 cm flux index (F10.7); geomagnetic K index

1 Introduction

The ionosphere is an important part of near the earth space environment and the mesosphere is the coldest region in the earth's atmosphere at local summer time. Polar Mesosphere Summer Echoes (PMSE) are strong echoes detected by radars from medium frequency (MF) to ultra-high frequency (UHF) bands in

polar summer mesopause, and PMSE has been considered to be possible indicators of global change (Thomas and Olivero, 2001). Its strongest average echo occurs at the altitude of about 86 km, and the observation range is 75-100 km (Czechowsky et al., 1979). Radar waves in the very high frequency (VHF) band are backscattered by irregularities of the electron density with spatial scales of about half the radar

5   wavelength: this was recently confirmed by Blix et al. from simultaneous rocket and radar observations (Blix et al., 2003). These polar mesospheric summer echoes (PMSE) are fundamentally related to the ice particles in mesospheric ice clouds (Rapp and Lübken, 2004). Even though this theory has been presented incompletely, it still provided a great impetus for the research of PMSE generation mechanism. The most extensively accepted theory is that the electron diffusion was characterized by the slowest ambipolar

10 diffusion mode associated with the charged ice grains (Cho et al., 1992). Varney et al. (2011) scrutinized one particular aspect of the turbulent theory of PMSE: the electron density dependence of the echo strength.

   Palmer et al. (1996) presented a statistical study of PMSE, after analyzed the observations of the EISCAT VHF radar during 1988–1993. They confirmed that: (1) these echoes are a summer phenomenon,

15 lasting from June to August; (2) PMSE occur mostly around noon and midnight, following a semidiurnal pattern; (3) the echoing structures move bodily, perhaps in response to gravity waves. Bremer et al. (2003) derived that the variation of PMSE is markedly controlled by solar cycle variations and precipitating high energetic particle fluxes based on measurements at 53.5 MHz in Andenes, Norway, with the ALOMAR SOUSY radar during 1994-1997 and with the ALWIN radar during 1999-2001. Bremer et al. (2006)

20 discussed that the strength of PMSE depends on the level of ionization because of the long-term changes of mesospheric summer echoes caused by the incident solar wave radiation and precipitating high energetic particle fluxes from about 20 May to the end of August during 1998–2006. Smirnova et al. (2010); Yi et al.(2017) found that inter-annual variations of PMSE OR (occurrence ratio) and length of the season anticorrelate with solar activity represented by the solar 10.7 cm radio flux, and correlate with

25 geomagnetic activity represented by AP index based on ESRAD MST radar measurements in Kiruna, Sweden. Nevertheless, no statistically significant trends in PMSE occurrence ratio or in the length of the PMSE season were found in the paper. Smirnova et al. (2011) concentrated on the accurate calculation of PMSE absolute strength as expressed by radar volume reflectivity and found that inter-annual variations of PMSE volume reflectivity strongly correlate with the local geomagnetic K-index and

anticorrelate with solar 10.7 cm flux but did not find any statistically significant trend in PMSE volume reflectivity during 1997-2009. Li and Rapp (2011) reported that the correlations of the occurrence ratio of PMSE at 224 MHz with the solar and geomagnetic activities both show positive correlations. PMSE have been detected and widely studied based on long-term observations of many different MST

5 radars(Reid et al., 2013;Thomas et al., 1992;Smirnova et al., 2011) (Reid et al. 1989; Thomas et al. 1992; and Smirnova et al. 2011), since the first observation of PMSE in 1979, it is well-known that the observation results are different when PMSE are observed by different frequency radar even in the same sites, and PMSE often show obvious layered events.

Previous study by 53.5MHz radar has provided the basic characteristics, the short-term statistical

10 variations of PMSE and the relation among the PMSE, solar activity and geomagnetic activity detected. The correlation of PMSE at 224 MHz to the ionization level, however, is as significant as that of PMSE at 53.5 MHz to the ionization level, then it provides the basis and ideas for the research of 224MHz radar. There are still a few significant problems that must be solved with the characteristics of layered PMSE OR. Hence, it is necessary to analyze the PMSE layered OR and study layered PMSE characters deeply

15 with data measured by 224 MHz EISCAT VHF radar under different observation conditions. The statistical results of PMSE layered OR with the same radar at the same site over the period 2004-2015 are given in this paper, which was based on the experiment data detected by 224 MHz EISCAT VHF radar. In addition, the relationships of PMSE OR, geomagnetic K index and F10.7 are analyzed and discussed. The PMSE OR calculation method given in this paper solves the defect that the measurements

20 of EISCAT radar is discontinuous, which makes a significant breakthrough in the calculation and characterization of the PMSE layered OR detected by EISCAT radar and the results could provide definitive data foundation for further analysis and the investigation of the physical mechanism of PMSE.

2 radar and experiment data

The experiment data of PMSE was obtained by 224MHz EISCAT VHF radar from 2004 to 2015. The

25 radar is located at Tromsø, Norway (69.35°N, 19.14°E), and a cylindrical 120m×46m antenna, with beam-widths of 1.8° north-south and 0.6° east-west was used on it. It has frequency and phase modulation capability with pulse length of 1 μs to 2 ms. Furthermore, reliable information of the raw electron density about PMSE, which is not derived by analysis of the incoherent scatter spectrum, but power profiles or

near-zero-lag data can be obtained by EISCAT radar, and the level of electron density represents the

intensity of echoes. The parameters described in Table 1for accuracy control of EISCAT VHF radar.

EISCAT VHF radar ran several standard experiment modes: "manda, beata, bella, tau7, arcd

(arc_dlayer) and tau1". The main differences between the arcd and manda modes are illustrated in Table

5 2. The manda and arcd modes main used for low altitude detection, and provide spectral measurements

at mesospheric altitude. Therefore, the data used in this study is mainly given by manda and arcd modes.

The Grand Unified Incoherent Scatter Design and Analysis Program (GUISDAP) software package have

been used for analyzing the EISCAT VHF radar data. The electron density N_e analyzed by GUISDAP

software is obtained between 10^6 and 10^{14} m^{-3}.

10   . **Table 1** Parameters of the radars.

Radar	EISCAT VHF
Location	69.59º N 19.23º E
Operating frequency	224 MHz
Transmitter peak power	1.5 MW
Antenna 3-dB beam width	1.7º NS × 1.2º EW
Antenna effective area	5690 m^2
Pulse length (altitude resolution)	300 m
Pulse repetition frequency	741 Hz
No. of bits in code	64
No. of code permutations	128
No. of coherent integrations	1
Lag resolution	1.35 ms
Maximum lag	0.17 s

Table 2 EISCAT VHF radar standard experiments.

Name	Code length [bit]	Baud length [μs]	Sampling rate[μs]	Range span[km]	Time resolution [s]	Plasma line	Raw data
manda	61	2.4	1.2	19–209	4.8	-	Yes
arc_dlayer	64	2	2	60–139	5.0	-	-

3 Layered PMSE Occurrence ratios

PMSE occur in thin layers having thickness up to 3-4 kilometers, and the mean altitude distribution of
PMSE events is 80-90km. It is considered to be the area of independent abnormal echoes. Fig. 1 a), b)
and c) show the typical events of PMSE monolayer, double-layer and tri-layer, respectively. One

5   remarkable feature of all PMSE is the fact that the radar echoes often occur in the form of two or more
distinct layers that can persist for periods of up to several hours. Until now, the layering-mechanism
leading to these multiple structures is not well understood. Here we are studying the occurrence of these
multiple layer events and its relationship with solar and geomagnetic activity. This content will be
discussed in detail later in the article.
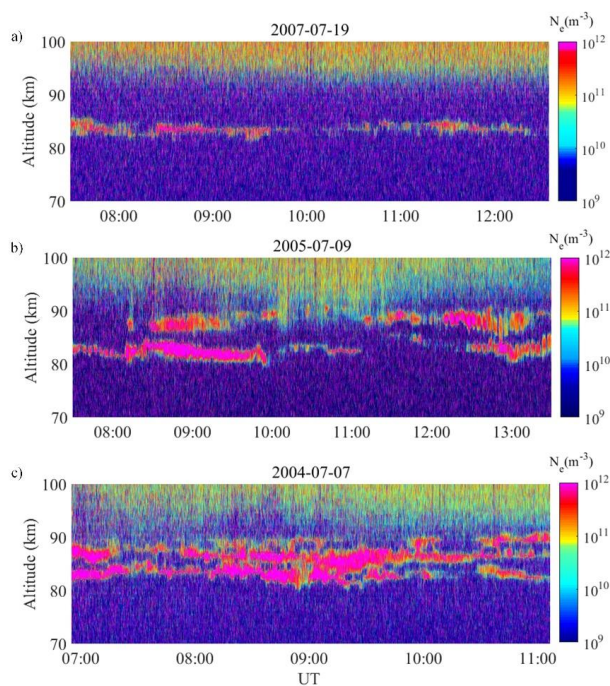
**Fig. 1 The typical layered PMSE events observed by EISCAT 224MHz VHF radar. a) The observation on 19
July, 2007 (Upper panel); b) The observation on 9 July, 2005 (Middle panel); c) The observation on 7 July,
2004 (lower panel). The red circle marks the obvious layered phenomenon of PMSE events.**

3.1 Calculation method

To find the characteristic of PMSE occurrence ratio (OR), a computing method and threshold must be defined. First of all, the data during radar heating experiments has been eliminated. After that, the number of data points satisfying the threshold of electron density ($N_e > 2.6 \times 10^{11}$ m^{-3}) was calculated (Hocking

5   and Röttger ,1997). PMSE is not continuous in time, so if the number of data points satisfying the electron density threshold of PMSE were less than 8 data points in any time interval, these data points were replaced with the average of electron density (N_e) of 80-90 km regardless of the threshold (Rauf et al., 2018). It maintained the original electron density values at the corresponding time, so that the correlation is not influenced. The correlation coefficients have been calculated between PMSE OR and the 10.7cm

10   of the solar flux index (F10.7), PMSE OR and geomagnetic events K indices, respectively. Because we chose the integration time of manda and arcd models are 4.8s and 2s respectively, on the basis of the condition (t≥1 min), the PMSE is needed to be simultaneous for≥12 and 30 data points, respectively. What's more, some abnormal echoes are related to the precipitation particle areas are not considered to be PMSE and is neglected in later discussion.

15   The emphasis of this paper is to present a hybrid algorithm based on grid partitioning. The calculation method is based on time. Taking the calculation method of PMSE monolayer occurrence ratio as an example, the electron density detected by the EISCAT VHF radar are counted, and the electron density with the value larger than the threshold in this time period are taken out, and the ratio between the number of electron densities values during the monolayer PMSE sustained time and the number of electron

20   densities values during total observation time is obtained. At different heights, when an electron density value greater than the threshold and less than the threshold is continuously alternate observed in an observation region with altitude range from 3-4km, we believe that double-layer or multi-layer PMSE events occur. The PMSE double-layer OR is the ratio between the sustained time of PMSE double layer and the total observation time. The tri-layer OR is also calculated in this way.

25   ### 3.2 The variations of PMSE layered occurrence ratios

For studying the PMSE layered OR, PMSE layered occurrence time (OT) and total observing time detected by EISCAT VHF radar from 2004 to 2015 were illustrated in Table 3. PMSE mono- double- tri-layer and total OR were presented in Table 3 as well.

Table 3 Statistical data from 2004 to 2015.

Year	Total Observing Time/min	Monolayer PMSE OT/min	Double Layer PMSE OT/min	Triple layer PMSE OT/min	Monolayer OR	Double layer OR	Triple layer OR	Total OR
2004	16054	4701	2774	151	29.28%	17.28%	0.94%	47.50%
2005	8165	3564	1491	182	43.65%	18.26%	2.23%	64.14%
2006	9248	2950	910	93	31.78%	9.84%	1.01%	42.63%
2007	9341	3027	804	0	32.41%	8.61%	0.00%	41.02%
2008	3310	763	97	0	23.06%	2.92%	0.00%	25.98%
2009	2264	424	76	8	18.72%	3.34%	0.35%	22.41%
2010	6303	1799	498	53	28.54%	7.90%	0.84%	37.28%
2011	9638	3624	2692	202	37.60%	27.93%	2.10%	67.63%
2012	7497	3550	1554	207	47.35%	20.73%	2.76%	70.84%
2013	14037	6906	3873	532	49.20%	27.59%	3.79%	80.59%
2014	2971	998	731	64	33.60%	24.6%	2.15%	60.35%
2015	4776	2019	1022	22	42.28%	21.40%	0.46%	64.14%
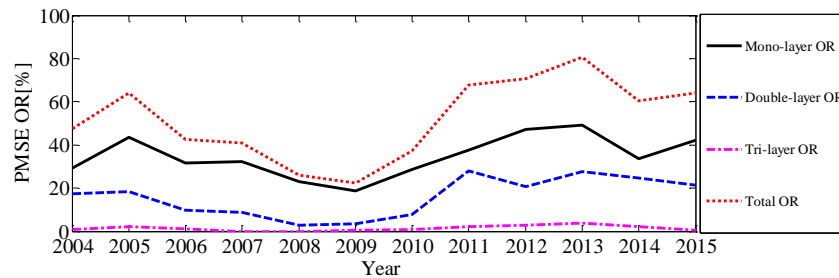
5   **Fig. 2 PMSE layered occurrence ratio. The OR of total (red dot line). The OR of monolayer (black solid line). The OR of double-layer (blue dashed line). The OR of triple -layer (pink dot-dashed line).**

Fig. 2 shows that the mono- double- and triple-layer OR agrees with the total PMSE OR. We calculated the Spearman rank correlation coefficients between mono-layer OR and double-layer OR, mono-layer

10   OR and tri-layer OR, mono-layer OR and Total OR, respectively. The correlation coefficients (r_s) are 0.7922, 0.7718 and 1 reached very significant level($P<0.05$), respectively. In addition, the PMSE layered OR from 2008 to 2010 is relatively low, and the solar activity was relative 'quiet' in these years.

Two significant phenomena can be discovered from Fig. 2: One was the layered OR of PMSE is different but regular. That is, the OR of monolayer is the highest, double-layer lies in the middle and the triple-layer is the lowest; The other was PMSE layered and total OR values show similar shape of sinusoidal, which has obvious wave peak and wave valley. One wave peak lies in the year about 2005,

5 the other lies in the year 2013. The values of two wave peaks are different, and the values in 2005 are smaller than that 2013. The values of wave valley lie in 2008-2009. Meanwhile, the gap between two peaks of PMSE OR is about 7 or 8 years. Here we only give the results of the data analysis, no longer do the cause analysis, because the stratification of PMSE is affected by many factors and has yet to be decided. The analyzing method and the results drawn during the process of this paper have a certain

10 reference value for right and in depth researching the PMSE.

3.3 Seasonal behaviour

The mean seasonal variations of the PMSE layered OR and PMSE total OR observed by EISCAT VHF radar during 2004-2015 were shown in Fig. 3 and Fig. 4, respectively. It illustrated the mean seasonal variation of the mono- (blue bars) double- (yellow bars) and tri-layer (red bars) PMSE OR and a

15 polynomial fit for the monolayer PMSE OR (black dot-curve) during 2004-2015. It can be derived from Fig. 3 and Fig. 4 that the monolayer PMSE events in the Tromsø, Norway, often begins in late May, reaches its maximum in early June or mid-June, keeps this level until the end of July or beginning of August, and gradually decreases or vanishes when it is close to the end of August or the beginning of September in general, which was in agreement with references(Smirnova et al., 2011). The double-layer

20 PMSE also begins in late May, but its maximum appears in mid-July. In addition, it keeps the larger value in June and July, and simply fade away in early August. The triple-layer PMSE appears a lot less in comparison to mono-, double- layer PMSE. In terms of time, it appears later and disappears earlier. What's more, the triple layer PMSE OR is large in end of June and early July, which is different than monolayer and double layer PMSE OR.

25 According to the statistical results, PMSE monolayer, double-layer and multilayer OR have seasonal variation. In addition, the trends of F10.7 and geomagnetic K index also fluctuates. Therefore, it is necessary to investigate the correlation of solar and geomagnetic activity on different layered PMSE OR during 2004-2015, and better explain the mechanism of PMSE. It is well known that other missions apart

from PMSE regular observations are performed by EISCAT VHF radar, so EISCAT radar does not provide continuous PMSE observations. Just by noting that there have a few deviations by methods of calculating layered PMSE OR, we raise an important question: Table 3 indicates a difference in total observation time for the individual years. How has this been taken into account for the determination of

5 occurrence ratios? Therefore, we use another method to recalculate the PMSE layered OR. Then the correlation between the PMSE layered OR and the F10.7 and between the PMSE layered OR and K index were studied. As mentioned in the calculation method section, we only select the days when PMSE is existed and calculate the layered occurrence ratio of PMSE.
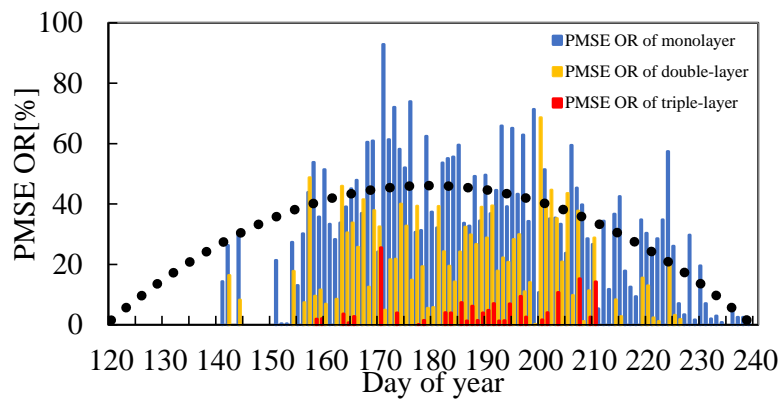
10 **Fig. 3 Mean seasonal variation of the PMSE mono-(in blue), double-(in yellow), triple-layer (in red) occurrence ratio at Tromsø using observations from 2004 to 2015.**
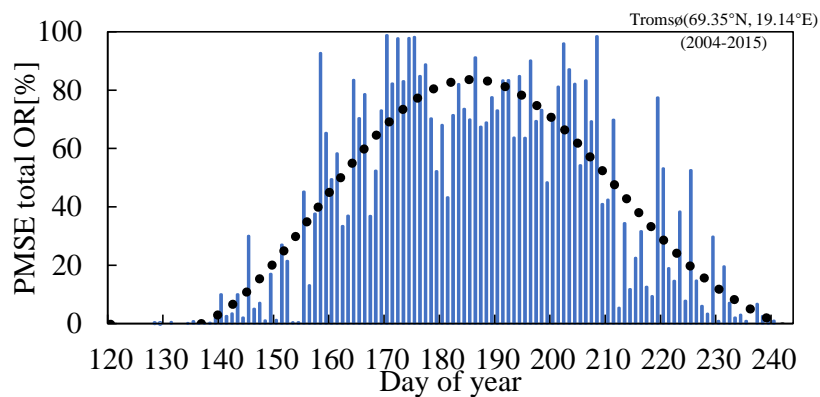
Fig. 4 Mean seasonal variation of the PMSE total occurrence ratio.

4 Discussion

We have calculated the PMSE layered OR and the relations among PMSE mono-, double- and triple-layer OR were analyzed statistically. At the same time, the mean seasonal variations of the layered PMSE OR and PMSE total OR were given. It is now generally accepted that both charged ice particles and

5   atmospheric turbulence play major roles in the change of the electron number density that lead to PMSE in the mesopause region (Rapp and Lübken, 2004). We know that solar and geomagnetic activities have a certain degree of influence on the occurrence of PMSE, but the effects of solar and geomagnetic activities on layered PMSE are not clear. Therefore, it is necessary to study the effects of solar and geomagnetic activities on layered PMSE. The occurrence ratio obtained by the ratio of the occurrence

10   time of PMSE to the total observation time is the calculation method in the traditional sense. It is easy to understand and accurately analyze the short-term variations, such as diurnal variation and seasonal variation of PMSE. However, the long-term trend is inaccurate by this calculation method, because the radar measurement data is not continuous. And it is difficult to discuss and analyze the relations between PMSE and solar activities and between PMSE and geomagnetic activities. Therefore, we have designed

15   a new calculation method for calculating the PMSE layered occurrence ratio, which is based on the height. so that the occurrence of PMSE becomes continuous, and the long-term variations of PMSE becomes easy and relatively accurate. The relations between PMSE and solar activities and between PMSE and geomagnetic activities can be studied.

4.1 Calculation method

20   The calculation method is based on altitude. A large number of literatures and experimental observations shown that the altitude range of PMSE is 80-90km (Li and Rapp, 2011;Smirnova et al., 2010;Latteck and Bremer, 2013). Among all the altitude and electron density observed by EISCAT VHF radar, we only take the apparent electron density in the altitude range of 80-90km, and then take out the electron density greater than the threshold in the period when the PMSE is known to be present. The ratio between the

25   numbers of layered PMSE electron densities values greater than the threshold and the numbers of total electron density in the range of 80-90 km was calculated respectively. The double-layer and tri-layer PMSE OR obtained by this method have a higher occurrence ratio than the first method.
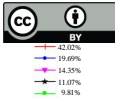
4.2 PMSE layered OR under different electron density threshold
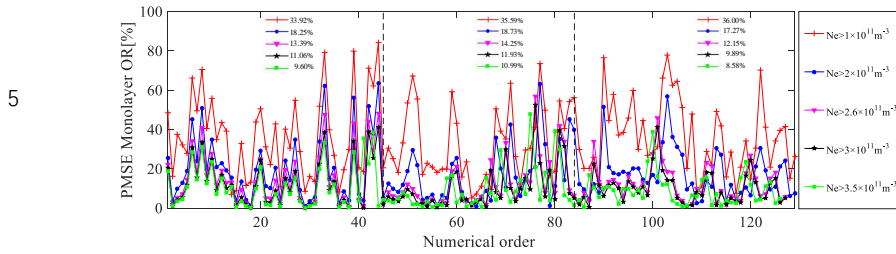
Fig. 5 PMSE monolayer occurrence ratio under different electron density threshold conditions. Vertical lines are the end of 2006 and 2011,respectively (black dashed line). The legends on the figure is the average of PMSE occurrence rate in three time periods separated by the black dashed line.
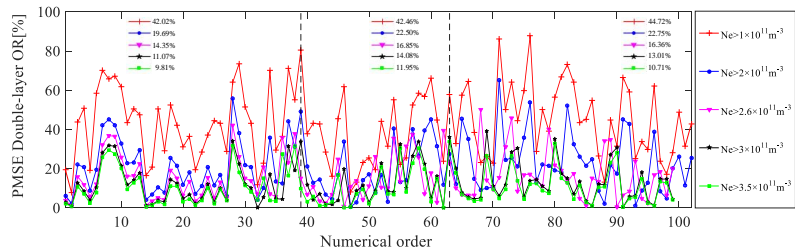
Fig. 6 PMSE double-layer occurrence ratio under different electron density threshold conditions. Vertical lines are the end of 2006 and 2011(black dashed line). The legends on the figure is the average of PMSE occurrence rate in three time periods separated by the black dashed line.
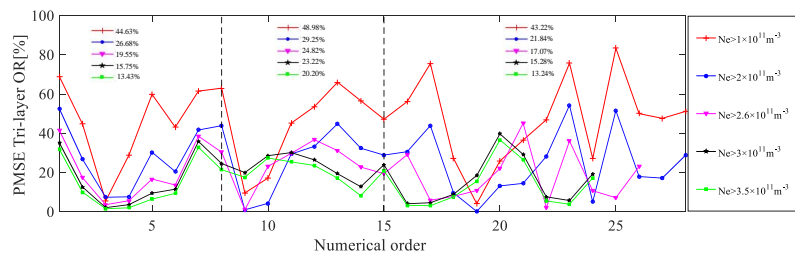
Fig.7 PMSE tri-layer occurrence ratio under different electron density threshold conditions. Vertical lines are the end of 2006 and 2011(black dashed line). The legends on the figure is the average of PMSE occurrence rate in three time periods separated by the black dashed line.

In this section, the day when the first occurrence of PMSE in 2004 (regardless of duration) was recorded as 1, and the day with the later occurrence of PMWE increased by sequence. Using this sequence as the horizontal axis and the PMSE layered OR with different electron density threshold as the vertical axis, the results are shown in Fig. 5, 6, and 7. That is, Fig. 5, Fig. 6 and Fig. 7 show PMSE mono- double- and

5   tri-layer OR under different electron density threshold conditions, respectively. In the calculation method section we said that we defined the electron density threshold ($N_e > 2.6 \times 10^{11} \mathrm{m}^{-3}$). Here, we give the PMSE layered OR with threshold conditions of $N_e > 1 \times 10^{11} \mathrm{m}^{-3}$, $N_e > 1.5 \times 10^{11} \mathrm{m}^{-3}$, $N_e > 2.6 \times 10^{11} \mathrm{m}^{-3}$, $N_e > 3 \times 10^{11} \mathrm{m}^{-3}$ and $N_e > 3.5 \times 10^{11} \mathrm{m}^{-3}$,respectively. We can get their variation trends to be largely consistent, in addition, the larger the threshold, the smaller the ratio. Since these occurrence ratios are

10   calculated in the case where the occurrence of PMSE is determined, there is no case of missing data, and it can be recognized that these occurrence rates are reliable. The legends on the figure is the average of PMSE mono-, double- and triple-layer OR with threshold conditions of $N_e > 1 \times 10^{11} \mathrm{m}^{-3}$, $N_e > 1.5 \times 10^{11} \mathrm{m}^{-3}$, $N_e > 2.6 \times 10^{11} \mathrm{m}^{-3}$, $N_e > 3 \times 10^{11} \mathrm{m}^{-3}$ and $N_e > 3.5 \times 10^{11} \mathrm{m}^{-3}$ during the periods of 2004-2006, 2007-2011 and 2012-2015. It is well known that 2006 is solar minimum and 2012 is solar maximum, but the PMSE

15   mono- and double-layer average OR is not consistent with solar activity. In other words, there has no correlation between PMSE mono- and double-layer OR and solar activity. What's more, we found that PMSE triple- layer OR and solar activity in opposite directions. To prove the conclusion, we will calculate the correlation coefficient between PMSE layered OR and solar activity and between PMSE layered OR and geomagnetic activity in next section. Therefore, the relation between them can be judged

20   directly.

4.3 Effect of solar and geomagnetic activity on PMSE OR

4.3.1 F10.7 index and K-index

The F10.7 index is a measure of the solar radio flux per unit frequency at a wavelength of 10.7 cm,

25   near the peak of the observed solar radio emission. F10.7 is often expressed in SFU or solar flux units (1 SFU = 10^{-22} W·m^{-2}·Hz^{-1}). It represents a measure of diffuse, nonradiative coronal plasma heating. It is an excellent indicator of overall solar activity levels and correlates well with solar UV emissions. The K-index quantifies disturbances in the horizontal component of earth's magnetic field with an integer in the

range 0-9 with 1 being calm and 5 or more indicating a geomagnetic storm. It is derived from the

maximum fluctuations of horizontal components observed on a magnetometer during a three-hour

interval. The K-index was introduced by Julius Bartels in 1938(Bartels et al., 1939). The K index values

used in the paper is the median of the K index observed on a magnetometer during a day, which has

5   removed the effects of the heating experiment.

4.3.2 Correlation coefficients

A correlation coefficient is a numerical measure of some type of correlation, meaning a statistical

relationship between two variables (Boddy and Smith, 2009). The Pearson correlation coefficient known

as Pearson's *r*, is a measure of the strength and direction of the linear relationship between two variables

10   that is defined as the covariance of the variables divided by the product of their standard deviations. This

is the best known and most commonly used type of correlation coefficient. Pearson's correlation

coefficient Given a pair of random variables (X, Y), the formula for *r* is (Wilks, 1995):

$$r_{X,Y} = \frac{\text{cov}(X,Y)}{\sigma_X \sigma_Y}$$

Where:

15   *Cov* is the covariance.

σ_X is the standard deviation of X

σ_Y is the standard deviation of *Y*.

Spearman's rank correlation coefficient is a measure of how well the relationship between two variables

can be described by a monotonic function. The Spearman correlation between two variables is equal to

20   the Pearson correlation between the rank values of those two variables. While Pearson's correlation

assesses linear relationships, Spearman's correlation assesses monotonic relationships (whether linear or

not) (Well and Myers, 2003). For a sample of size *n*, the *n* raw scores X_i, Y_i are converted to ranks rgX_i,

rgY_i, and r_s is computed from:

$$r_S = \frac{\text{cov}(rg_X, rg_Y)}{\sigma_{rg_X} \sigma_{rg_Y}}$$

25   Where:

$\text{cov}(rg_X, rg_Y)$ is the covariance of the rank variables.

σ_{rg_X} and σ_{rg_Y} are the standard deviations of the rank variables.

A high value (approaching +1.00) is a strong direct relationship, values near 0.50 are considered moderate and values below 0.30 are considered to show weak relationship. A low negative value (approaching -1.00) is similarly a strong inverse relationship, and values near 0.00 indicate little, if any relationship.

5   **4.3.3 Correlation between layered PMSE OR, F10.7 and K index**
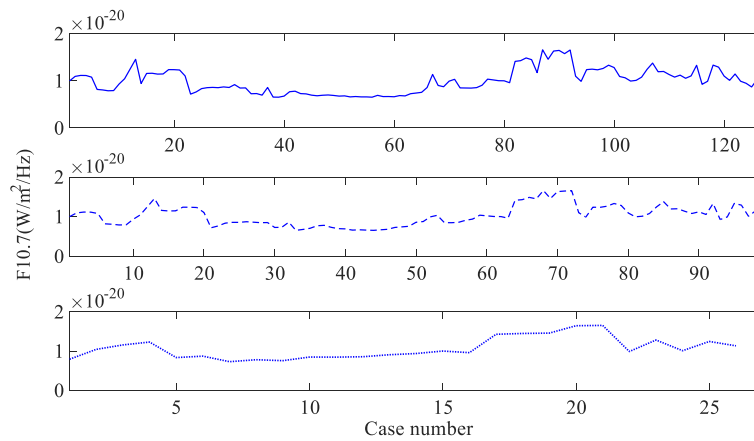
(a)
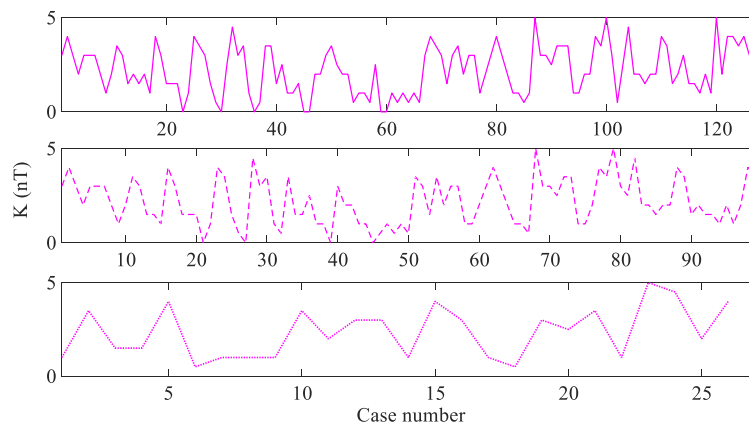
(b)

10   **Fig. 8 (a) The variations of F10.7 values corresponding to the occurrence of PMSE. Upper panel: F10.7 values corresponding to the occurrence of mono-layer PMSE; Middle panel: F10.7 values corresponding to the occurrence of double-layer PMSE; lower panel: F10.7 values corresponding to the occurrence of triple-layer PMSE. (b) The variations of geomagnetic K index values corresponding to the occurrence of PMWE.**

15   **Upper panel: K index values corresponding to the occurrence of mono-layer PMSE; Middle panel: K index**

values corresponding to the occurrence of double-layer PMSE; lower panel: K index values corresponding to the occurrence of triple-layer PMSE.
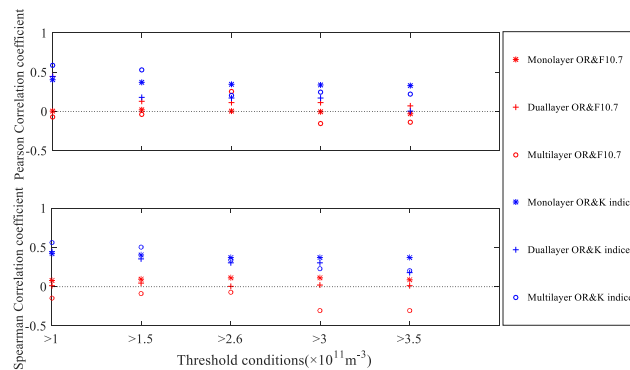
5 **Fig. 9 Pearson linear and Spearman rank correlation computed between layered PMSE OR (with threshold conditions of $N_e > 1 \times 10^{11} \text{m}^{-3}$, $N_e > 1.5 \times 10^{11} \text{m}^{-3}$, $N_e > 2.6 \times 10^{11} \text{m}^{-3}$, $N_e > 3 \times 10^{11} \text{m}^{-3}$ and $N_e > 3.5 \times 10^{11} \text{m}^{-3}$, respectively) and F10.7 corresponding to the occurrence of PMSE and between layered PMSE OR and K index corresponding to the occurrence of PMSE, respectively. For each correlation coefficient, P value is less than 0.05. The horizontal dotted line is drawn to separate positive and negative correlation coefficients.**

10 Fig.8 shows that the variations of F10.7 and geomagnetic K index values corresponding to the occurrence of PMSE. The F10.7 and K values corresponding to the occurrence of PMSE with threshold conditions of $N_e > 2.6 \times 10^{11} \text{m}^{-3}$. Combined with Fig. 5, 6, and 7, we can roughly analyze the relationship between the layered PMSE OR and the F10.7 and between the layered PMSE OR and K values, but the results may be relatively inaccurate. In order to study the correlation between layered PMSE OR and F10.7 and

15 between layered PMSE OR and K index, all the data points of PMSE OR, F10.7 and K index with simultaneous occurrence were combined. Fig.9 shows the correlation coefficients computed by combing all the points of PMSE OR (with threshold conditions of $N_e > 1 \times 10^{11} \text{m}^{-3}$, $N_e > 1.5 \times 10^{11} \text{m}^{-3}$, $N_e > 2.6 \times 10^{11} \text{m}^{-3}$, $N_e > 3 \times 10^{11} \text{m}^{-3}$ and $N_e > 3.5 \times 10^{11} \text{m}^{-3}$), F10.7 and K index with simultaneous occurrence and apply significant test. It can be seen from Fig.9 that layered PMSE OR is positively correlated with the

20 K index, but the correlation coefficient between PMSE mono- and F10.7, double-layer OR and F10.7 both are very low, indicating that their correlation is weak or even not relevant. Interestingly, we found that the PMSE tri-layer OR has a negative correlation with F10.7, this finding has never published in any existing literature. Hence, it is indicated that the cases with positive values play a decisive role when calculating the correlation coefficient between the data points of PMSE and K occur simultaneously, and

events with negative values dominate in the calculation of the correlation coefficient between PMSE tri-layer OR and F10.7. But PMSE mono-, double- layer OR has hardly relevance with F10.7.

The correlation between PMSE layered OR and F10.7 and between PMSE layered OR and K index were obtained. It indicates that there are many complicated factors for the formation and development of

5   PMSE besides the solar and geomagnetic activities. There are explanations for these results: on one hand, the enhanced solar activity increases the electron density due to the increase of ionization, and with the increase of solar radiation, the photodissociation enhance and the water vapor content is reduced. On the other hand, the positive correlation between PMSE OR and K index may be apprehensible as because of the enhanced magnetic activity caused precipitating particles increase in the mesosphere, and lead to

10   increase in electron densities. But I still can't explain why there is a negative correlation between tri-layer PMSE OR and F10.7, or this may be our future research focus.

5 Conclusions

In the paper, we presented PMSE occurrence ratios with monolayer, double- and triple- layers that were detected by EISCAT VHF radar during a solar cycle. It was obtained that the daily variation and seasonal

15   variation of the layered PMSE. We implemented a new method to provide more accurate conclusions on the study of the long-term variation of PMSE with different thresholds. Then the relationship between layered PMSE and solar radiation flux (F10.7) and between layered PMSE and geomagnetic activity (K index) were given. The following conclusions were reached:

(1)   Mono-, double- and tri-layer PMSE have different seasonal behavior. Monolayer PMSE events

20   often begins in late May, reaches its maximum in early June or mid-June, keeps this level until the end of July or beginning of August, and gradually decreases or vanishes when it is close to the end of August or the beginning of September in general, which was in agreement with references (Smirnova et al., 2011). The double-layer PMSE reaches its maximum appears in mid-July and simply fade away in early August. The triple-layer PMSE appears later and disappears earlier in comparison to mono-, double-

25   layer PMSE, and it is large in end of June and early July.

(2)   The variation trends of PMSE mono- double- and tri-layer OR under different electron density threshold conditions are largely consistent. It was got that the larger the threshold, the smaller the ratio.

Beyond that, PMSE mono- and double-layer OR were not associated with solar activity. and PMSE triple- layer OR is inversely proportional to solar activity.

(3)   PMSE layered OR is positively correlated with the K index. The correlation between PMSE mono- and double- layer OR and F10.7 is relatively weak, and PMSE tri-layer OR has a negative correlation with F10.7.

Acknowledgments

This study is supported by the National Natural Science Foundation of China [No. 41104097 and No.41304119]. This study is also supported by the National Key Laboratory of Electromagnetic Environment, China Research Institute of Radiowave Propagation (CRIRP). We also acknowledge EISCAT, which is an international association supported by China, Finland, Japan, Norway, Sweden, and the UK.

References

Bartels, J., Heck, N. A. H., and Johnston, H. F.: The Three-Hour-Range Index Measuring Magnetic Activity, Journal of Geophysical Research, 44, 411-454, doi.org/10.1029/TE044i004p00411, 1939.

Blix, T. A., Rapp, M., and Lübken, F. J.: Relations between small scale electron number density fluctuations, radar backscatter, and charged aerosol particles, Journal of Geophysical Research Atmospheres, 108, 1-10, doi:org/10.1029/2002JD002430, 2003.

Boddy, R., and Smith, G.: Statistical Methods in Practice: for Scientists and Technologists, John Wiley & Sons Ltd Chichester, 2009.

Bremer, J., Hoffmann, P., Latteck, R., and Singer, W.: Seasonal and long-term variations of PMSE from VHF radar observations at Andenes, Norway, Journal of Geophysical Research Atmospheres, 108, doi:org/10.1029/2002JD002369, 2003.

Bremer, J., Hoffmann, P., Höffner, J., Latteck, R., Singer, W., Zecha, M., and Zeller, O.: Long-term changes of mesospheric summer echoes at polar and middle latitudes, Journal of Atmospheric and Solar-Terrestrial Physics, 68, 1940-1951, doi:org/10.1016/j.jastp.2006.02.012, 2006.

Cho, J. Y. N., Hall, T. M., and Kelley, M. C.: On the Role of Charged Aerosols in Polar Mesosphere Summer Echoes, Journal of Geophysical Research Atmospheres, 97, 875-886, doi:org/10.1029/91JD02836, 1992.

Czechowsky, P., Ruester, R., and Schmidt, G.: Variations of mesospheric structures in different seasons,

5 Geophysical Research Letters, 6, 459-462, doi:org/10.1029/GL006i006p00459, 1979.

Hocking, W. K., and Röttger, J.: Studies of polar mesosphere summer echoes over EISCAT using calibrated signal strengths and statistical parameters, Radio Science, 32, 1425-1444, doi:org/10.1029/97RS00716, 1997.

Latteck, R., and Bremer, J.: Long-term changes of polar mesosphere summer echoes at 69°N, Journal of

10 Geophysical Research Atmospheres, 118, 10441-10448, doi:10.1002/jgrd.50787, 2013.

Li, Q., and Rapp, M.: PMSE-observations with the EISCAT VHF and UHF-radars: Statistical properties, Journal of Atmospheric and Solar-Terrestrial Physics, 73, 944-956, doi:org/10.1016/j.jastp.2010.05.015, 2011.

Palmer, J. R., Rishbeth, H., Jones, G. O. L., and Williams, P. J. S.: A statistical study of polar mesosphere

15 summer echoes observed by EISCAT, Journal of Atmospheric and Solar-Terrestrial Physics, 58, 307-315, doi:org/10.1016/0021-9169(95)00038-0, 1996.

Rapp, M., and Lübken, F. J.: Polar mesosphere summer echoes (PMSE): review of observations and current understanding, Atmospheric Chemistry and Physics, 4, 2601-2633, doi:org/10.5194/acp-4-2601-2004, 2004.

20 Rauf, A., Li, H., Ullah, S., Meng, L., Wang, B., and Wang, M.: Statistical study about the influence of particle precipitation on mesosphere summer echoes in polar latitudes during July 2013, Earth Planets and Space, 108(70), doi:org/10.1186/s40623-018-0885-6, 2018.

Smirnova, M., Belova, E., Kirkwood, S., and Mitchell, N.: Polar mesosphere summer echoes with ESRAD, Kiruna, Sweden: Variations and trends over 1997–2008, Journal of Atmospheric and Solar-

25 Terrestrial Physics, 72, 435-447, doi:10.1016/j.jastp.2009.12.014, 2010.

Smirnova, M., Belova, E., and Kirkwood, S.: Polar mesosphere summer echo strength in relation to solar variability and geomagnetic activity during 1997–2009, Annales Geophysicae, 29, 563-572, doi:10.5194/angeo-29-563-2011, 2011.

Thomas, G. E., and Olivero, J.: Noctilucent clouds as possible indicators of global change in the mesosphere, Advances in Space Research, 28, 937-946, 2001.

Varney, R. H., Kelley, M. C., Nicolls, M. J., Heinselman, C. J., and Collins, R. L.: The electron density dependence of polar mesospheric summer echoes, Journal of Atmospheric and Solar-Terrestrial Physics,

5   73, 2153-2165, doi:org/10.1016/j.jastp.2010.07.020, 2011.

Well, A. D., and Myers, J. L.: Research design and statistical analysis, New York, 1-736, 2003.

Wilks, D. S.: Statistical Methods in the Atmospheric Sciences, Burlington, MA: Academic Press, 1995.

Yi, W., Reid, I. M., Xue, X., Younger, J. P., Murphy, D. J., Chen, T., and Dou, X.: Response of neutral mesospheric density to geomagnetic forcing, Geophysical Research Letters, 44, 8647-8655,

10   doi:org/10.1002/2017GL074813, 2017.